CrossMark

ORIGINAL ARTICLE

Pinus radiata bark extract induces caspase-independent apoptosis-like cell death in MCF-7 human breast cancer cells

Thamizhiniyan Venkatesan · Young-Woong Choi · Sung-Phil Mun · Young-Kyoon Kim

Abstract In the present study, we investigated the anticancer activity of *Pinus radiata* bark extract (PRE) against MCF-7 human breast cancer cells. First, we observed that PRE induces potent cytotoxic effects in MCF-7 cells. The cell death had features of cytoplasmic vacuolation, plasma membrane permeabilization, chromatin condensation, phosphatidylserine externalization, absence of executioner caspase activation, insensitivity to z-VAD-fmk (caspase inhibitor), increased accumulation of autophagic markers, and lysosomal membrane permeabilization (LMP). Both the inhibition of early stage autophagy flux and lysosomal cathepsins did not improve cell viability. The antioxidant, *n*-acetylcysteine, and the iron chelator, deferoxamine, failed to restore the lysosomal integrity indicating that PRE-induced LMP is independent of oxidative stress. This was corroborated with the absence of enhanced ROS production in PRE-treated cells. Chelation of both intracellular calcium and zinc promotes PRE-induced LMP. Geranylgeranylacetone, an inducer of Hsp70 expression, also had no significant protective effect on PRE-induced LMP.

Moreover, we found that PRE induces endoplasmic reticulum (ER) stress and mitochondrial membrane depolarization in MCF-7 cells. The ER stress inhibitor, 4-PBA, did not restore the mitochondrial membrane integrity, whereas cathepsin inhibitors demonstrated significant protective effects. Collectively, our results suggest that PRE induces an autophagic block, LMP, ER stress, and mitochondrial dysfunction in MCF-7 cells. However, further studies are clearly warranted to explore the exact mechanism behind the anticancer activity of PRE in MCF-7 human breast cancer cells.

Keywords Anticancer source · Autophagic inhibitor · Breast cancer · Lysosomal membrane permeabilization · *Pinus radiata* · Polyphenols

T. Venkatesan · Y.-W. Choi · Y.-K. Kim (✉)
Department of Forest Products and Biotechnology, College of Forest Science, Kookmin University, 861-1 Chongnung-dong, Songbuk-gu, Seoul 136-702, South Korea
e-mail: ykkim@kookmin.ac.kr

URL: http://www.kookmin.ac.kr
S.-P. Mun
Department of Wood Science and Technology, College of Agriculture and Life Science, Chonbuk National University, Jeonju 561-756, South Korea

Introduction

Despite the fact that surgery is usually the first line of attack against breast cancer, tumor recurrence is the most common risk even after successful surgical resection of the primary tumor (Howell 2004). In such case, the best option for breast cancer treatment is the use of chemotherapies.

Studies have clearly demonstrated that cancer cells are more significantly dependent on autophagy for survival than noncancerous cells (Apel et al. 2008; Livesey et al. 2009). Autophagy is a self-protective mechanism that functions to maintain cellular homeostasis during brief periods of starvation and in the presence of various

metabolically stressful stimuli (Heymann 2006). Numerous studies have shown that the pharmacological or genetic inhibition of the autophagic process could significantly reduce the growth and viability of cancer cells (Racoma et al. 2013). On the other hand, prolonged, increased activation of the autophagic process has also been reported to induce cancer cell death; excessive autophagy leads to the destruction of functional proteins and other important signaling molecules, which eventually causes cellular damage and death (Amelio et al. 2011). Hence, either the inhibition or the activation of autophagy might be a promising strategy for cancer treatment.

Lysosomes are the major intracellular digestive compartment involved in many cellular processes including autophagy. During autophagy, cellular components such as damaged proteins and organelles are transported to lysosomes for degradation and recycling of molecules for anabolic processes. Therefore, lysosomes are considered a crucial regulator of cellular homeostasis (Appelqvist et al. 2013). It is believed that lysosomes in cancer cells are more susceptible to lysosomal membrane permeabilization (LMP) inducers as they are larger in size compared to normal cells (Boya and Kroemer 2008). Following LMP, lysosomal enzymes are released into the cytoplasm and induce cell death either via mitochondrial dependent or independent pathways. Lysosomotropic agents are weak bases that diffuse across membranes and become trapped within the acidic lysosomes after protonation and cause lysosomal membrane damage owing to their detergent-like properties (Aits and Jäättelä 2013). The in vivo study in mouse models of fibrosarcoma and breast cancer clearly demonstrated the antitumorigenic activity of the lysosomotropic agent, siramesine (Ostenfeld et al. 2005). Further, the naturally occurring polyphenolic compounds like pterostilbene and the well-known anticancer alkaloids such as vincristine, vinblastine, and paclitaxel have also been reported to induce cell death via LMP (Mena et al. 2012; Boya and Kroemer 2008).

Perturbation of ER homoeostasis due to the accumulation of misfolded and/or unfolded proteins in the ER lumen, as a result of disturbed calcium homoeostasis and redox status, leads to the activation of an evolutionarily conserved cellular response known as unfolded protein response (UPR) or ER stress response. Usually, the primary biological goal of the UPR is to re-establish the normal function of the ER. However, persistent ER stress and UPR activation can switch the cytoprotective functions of UPR into toxic responses (Sano and Reed 2013).

Cancer cells are known to have higher levels of ER stress than normal cells due to their altered metabolic rates (Yadav et al. 2014). Therefore, promotion of this already engaged ER stress in cancer cells is considered an alternative approach for cancer treatment. In the recent past, many natural compounds with the ability to induce ER stress have been identified and transformed to clinical trials in order to treat various cancer types (Trondl et al. 2014).

As a large group of bioactive substances, phenolic compounds have the ability to target cancer cells by various mechanisms (Chen et al. 2014; Hasima and Ozpolat 2014; Suganuma et al. 2006; Weng and Yen 2012). Here we report that PRE, the polyphenolic-rich, bioactive, ethanolic subfraction of *Pinus radiata* bark extract, induces caspase-independent, apoptosis-like cell death in MCF-7 human breast cancer cells with the involvement of an autophagic block, LMP, ER stress, and mitochondrial dysfunction.

Materials and methods

Reagents and antibodies

The autophagic inhibitors 3-methyladenine (3-MA) and bafilomycin A1 (BafA1) were purchased from Sigma-Aldrich (St. Louis, MO, USA) and Santa Cruz Biotechnology, Inc. (Dallas, TX, USA), respectively. The broad spectrum caspase inhibitor z-VAD-fmk was from Calbiochem. The cathepsin inhibitors CA-074Me and pepstatin-A, *n*-acetylcysteine (NAC), deferoxamine mesylate (DFO), geranylgeranylacetone (GGA), staurosporine, Hoechst 33342, propidium iodide (PI), N,N,N',N'-tetrakis(2-pyridylmethyl)ethylenediamine (TPEN), 1,2-bis(2-aminophenoxy)ethane-N,N,N',N'-tetraacetic acid tetrakis(acetoxymethyl ester) (BAPTA-AM), H_2DCF-DA, and the antibody for LC3 were procured from Sigma-Aldrich (St. Louis, MO, USA). The antibodies for GRP78, LAMP-1, cathepsin-D, GAPDH, and HRP-conjugated secondary antibodies were from Santa Cruz Biotechnology, Inc. (Dallas, TX, USA). Antibodies for IRE1α, phospho-eIF2α, CHOP, p62, and caspase-7 were from Cell Signaling Technology (Beverly, MA, USA).

Extraction and fractionation

Ten grams of *P. radiata* bark powder (1 mm pass) and 100 ml of deionized water were put into a 500-ml round

bottom flask. The contents in the flask were heated on PEG#400 bath preset to 110 °C for 1 h with occasional shaking. Afterwards, the bark slurry was filtered using a 17G3 glass filter and the residue was washed with hot water. The filtrate and washings were combined and the volume was adjusted to 400 ml with deionized water. We abbreviated this solution as HWE (hot water extract). HWE was passed through Diaion HP20 column (3.2 × 21 cm) for 3 h and then the column was completely washed with deionized water. Next, the column was maintained at 90 °C for the elution of adsorbed molecules using water followed by 95 % ethanol. The desorbed aqueous (*P. radiata* aqueous fraction, PRA) and ethanolic (*P. radiata* ethanolic fraction, PRE) fractions were concentrated and evaluated for their cytotoxic effects against MCF-7 human breast cancer cells. The PRE demonstrated potent cytotoxic effects in MCF-7 human breast cancer cells. However, PRA did not influence the cancer cell viability, up to a concentration of 200 μg/ml (data not shown). Thus, we chose to study PRE to further evaluate the anticancer activity of *P. radiata* bark extract.

Cell line and culture conditions

The human breast cancer cell line, MCF-7, was purchased from the Korean Cell Line Bank (KCLB), South Korea. Cells were grown in Dulbecco's modified Eagle's medium (DMEM) supplemented with 10 % fetal bovine serum (FBS) and antibiotics. Cultures were maintained at 37 °C in a humidified atmosphere with 5 % CO_2. Cells were passaged twice per week to maintain logarithmic growth. Cells were plated and allowed to adhere for 24 h. Then, cells were treated with extracts in DMEM containing 1 % FBS with no antibiotics nor phenol red.

Cell viability assay

The cytotoxic effect of PRE on breast cancer cells was determined by the trypan blue dye exclusion method, as described previously with some modifications. Briefly, cells were seeded into six-well plates at a density of $2 × 10^5$ cells per ml and maintained on media for 24 h. Cells were then treated with desired concentrations of PRE for 24 h. Afterwards, cells were trypsinized, and the percentage of viable cell numbers was counted by the trypan blue dye exclusion method using a hemocytometer. The influence of various inhibitors on PRE-

induced cytotoxicity on breast cancer cells was also determined by the same method.

Flow cytometric analysis

Annexin V-FITC/PI staining was used to assess apoptosis and necrosis in MCF-7 cells according to the manufacturer's instructions. Briefly, cells were seeded into six-well plates and treated with PRE for 24 h. Then, cells were trypsinized, washed with PBS, and suspended in annexin binding buffer at a density of $1 × 10^6$ cells per ml. One hundred microliters of cell suspension from each sample was aliquotted into sterile Eppendorf tubes, to which 5 μl of annexin V-FITC antibody and 5 μl of propidium iodide (BD Biosciences, San Jose, CA) were added and incubated for 15 min at RT. Afterwards, for a total volume of 500 μl, annexin binding buffer was added. Then, they were analyzed using a flow cytometer.

To assess the integrity of lysosomes, cells were harvested, stained with 100 nM of LysoTracker Green DND-26 (Life Technologies), and then analyzed by flow cytometry. The integrity of the ER and the mitochondrial membrane potential were also analyzed by flow cytometry using ER-Tracker Blue-White DPX dye (Life Technologies) and MitoTracker Red (Santa Cruz Biotechnology, Inc.), respectively.

Phase-contrast and fluorescence microscopy

To examine the morphological changes, cells were treated with PRE for 24 to 48 h. After being rinsed with fresh medium, the cells were visualized and imaged under a phase-contrast microscope.

The effect of PRE on lysosomal membrane integrity was analyzed by immunofluorescence staining of lysosomal protease, cathepsin-D. Briefly, cells were grown on poly-l-lysine-coated glass coverslips placed in six-well plates and treated with PRE for 24 h. Then, cells were fixed using 4 % paraformaldehyde and permeabilized with 0.2 % Triton-X 100 in PBS for 10 min followed by PBS washes. After blocking with PBS containing 2 % BSA, cells were incubated with rabbit anti-cathepsin-D antibody (SC-10725) in Tris-buffer saline with 0.05 % Tween-20 (T-TBS) containing 2 % BSA. Cells were incubated overnight at 4 °C. After T-TBS washes, cells were incubated with Alexa Fluor 488-conjugated, goat anti-rabbit IgG for 1 h in the dark. Nuclei were stained with DAPI and cells were washed

with T-TBS. Coverslips were mounted using a drop of mounting medium on the glass slides and sealed with nail polish to prevent drying and movement under a microscope. Cells were visualized and images were captured under fluorescence microscopy.

Western blot analysis

Cells were initially seeded at a density of 2×10^5 cells per ml in a 100-mm dish and grown in the medium for 24 h. Cells were then grouped and treated with PRE for 0–24 h. Afterwards, cells were lysed using a mammalian cell lysis buffer (CelLytic™ M, Sigma-Aldrich) supplemented with protease and phosphatase inhibitors (Roche Diagnostics). Lysates were clarified by centrifugation at 12,000 rpm for 15 min at 4 °C. For collection of the cytosolic fraction, cells were suspended in the extraction buffer consisting of 250 mM sucrose, 20 mM HEPES pH 7.5, 10 mM KCl, 1.5 mM $MgCl_2$, 1 mM EDTA, 1 mM EGTA, and 250 μg/ml digitonin with protease inhibitors (Roche). Samples were incubated on ice for 10 min, and vortexing was repeated and followed by centrifugation at 13,000 rpm at 4 °C for 1.5 min. The resultant supernatant was considered to be the cytosolic fraction and used for quantification of cathepsin-D as well as LAMP-1 for confirming the absence of lysosomes in the extracted cytosolic fraction. Protein concentration of the samples was determined using a BCA protein assay kit according to the manufacturer's instructions (Sigma-Aldrich), and samples were adjusted to contain equal protein concentrations using the same lysis buffer. Equal amounts of protein from each sample were then subjected to electrophoresis and proteins were transferred to a membrane using the Trans-Blot Turbo system (Bio-Rad). The membranes were blocked with 5 % milk or BSA for 1 h at room temperature and incubated in the primary antibody overnight with rocking at 4 °C. Following three washes in TBS-T, the membranes were incubated with the appropriate HRP-conjugated secondary antibody for 2 h at room temperature. Finally, the membranes were washed three times with TBS-T and examined by the chemiluminescence detection method.

Statistical analysis

Unless otherwise stated, data expressed as the mean ± SD from at least three independent experiments. Data were analyzed using the SPSS 16.0 student software (SPSS Inc, Chicago, IL). Statistical differences between groups were assessed using the one-way analysis of variance (ANOVA) followed by post hoc testing with a least significance difference test ($P < 0.05$).

Results

PRE induces cytoplasmic vacuolation-mediated cell death in MCF-7 human breast cancer cells

The cytotoxic effect of PRE on MCF-7 cells was analyzed by a trypan blue dye exclusion assay. As shown in Fig. 1a, PRE induces potent cytotoxic effects against MCF-7 cells in a dose-dependent manner. The IC_{50} value of PRE for MCF-7 cells was 64.79 μg/ml. The morphological changes in MCF-7 cells treated with PRE (IC_{50}) were observed under phase-contrast microscopy. PRE induces extensive cytoplasmic vacuolation in MCF-7 breast cancer cells, and we further observed that the progression of vacuolation was severe after 24 h treatment (Fig. 1b). These findings indicate that PRE induces cytoplasmic vacuolation-mediated cell death in MCF-7 human breast cancer cells.

PRE induces caspase-independent, apoptotic-like cell death in MCF-7 human breast cancer cells

Next, we set to determine the mode of cell death induced by PRE in MCF-7 breast cancer cells. To accomplish this, we first examined the plasma membrane integrity and nuclear morphological changes with propidium iodide and Hoechst 33342 staining. As shown in Fig. 2a, most of the cells in the PRE-treated group show condensed nuclei and loss of plasma membrane integrity. Majority of those cells were also annexin V-FITC positive (Fig. 2b). Staurosporine, a representative apoptotic inducer, activates caspase-7 in MCF-7 cells, whereas PRE had no effect on the caspase cascade (Fig. 2c). Furthermore, z-VAD-fmk, a broad spectrum caspase inhibitor, failed to reverse PRE-induced cell death (Fig. 2d), indicating PRE-induced MCF-7 breast cancer cell death is independent of caspases.

PRE blocks autophagic flux in MCF-7 human breast cancer cells

As cytoplasmic vacuolation is a common characteristic in processes like autophagy, paraptosis, necroptosis, and other cell death mechanisms (Wei et al. 2015), we first
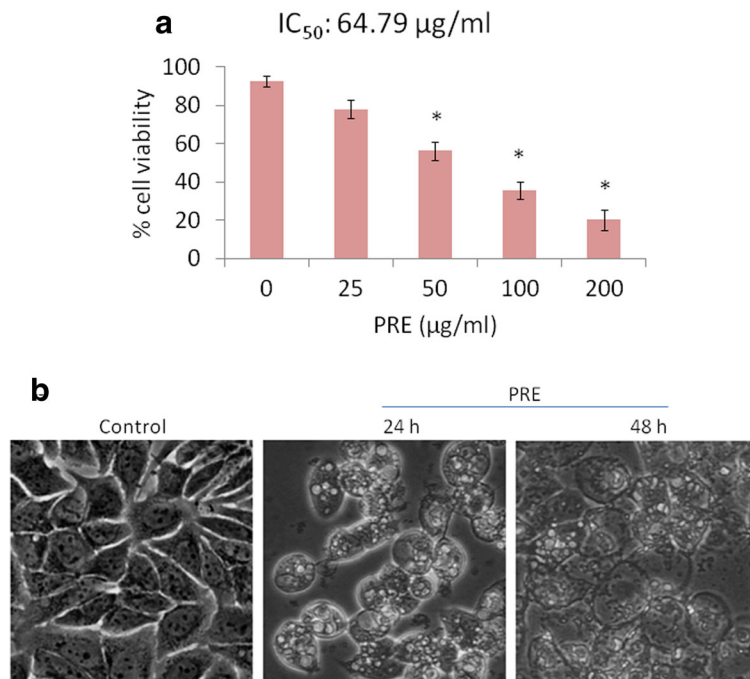
Fig. 1 Cytotoxic effect of PRE against MCF-7 human breast cancer cells. **a** PRE induces loss of breast cancer cell viability. MCF-7 cells were plated at a density of 2×10^5 cells per ml in six-well plates. After 24 h, the medium was replaced with fresh medium containing 1 % serum and the indicated concentration of PRE. Cell viability was determined by trypan blue dye exclusion method using a hemocytometer. Data are representative of three independent experiments. **b** PRE induces cytoplasmic vacuolation in MCF-7 breast cancer cells. To assess the morphological changes, cells were seeded into six-well plates and allowed to adhere overnight. Afterwards, cells were treated with PRE (65 µg/ml) for 24–48 h. Then cells were washed, visualized, and imaged under a phase-contrast microscope (×200). *P < 0.05 compared to control group

examined the effect of the autophagic inhibitor 3-MA on PRE-induced cytoplasmic vacuolation. Autophagy, an intracellular, self-degradative mechanism, begins with the formation of vacuoles known as autophagosomes around the intracellular cargo. Then, these autophagosomes fuse with lysosomes to degrade and recycle the engulfed cargo. 3-MA can block the formation of autophagic vacuoles via inhibition of class III PI-3K, which is known to be essential for induction of autophagy (Wu et al. 2010). As shown in Fig. 3a, 3-MA does not block the vacuolation induced by PRE. Despite 3-MA failing to block the vacuolation of MCF-7 cells, the accumulation of the autophagic marker protein, microtubule-associated protein 1 light chain 3 (LC3), was increased upon treatment with PRE (Fig. 3b). Furthermore, the levels of p62, a ubiquitin-binding protein, were also concomitantly increased in MCF-7 cells (Fig. 3b). During the autophagic process, p62 is transported to autophagosomes by direct interaction with LC3 and then degraded by lysosomal proteases (Komatsu and Ichimura 2010). When the fusion of autophagosomes with lysosomes is inhibited, the levels of p62 remain high due to the increased accumulation of autophagosomes (Bjørkøy et al. 2009). BafA1, a specific inhibitor of the vacuolar type H(+)-ATPase (V-ATPase), blocks the fusion of autophagosomes with lysosomes, thereby increasing the accumulation of LC3 and p62 during autophagic flux (Klionsky et al. 2008). As shown in Fig. 3c, BafA1 did not further increase the levels of LC3 and p62 in PRE-treated cancer cells. Moreover, the autophagic inhibitor 3-MA had no effect on PRE-induced breast cancer cell death (Fig. 3d). Taken together, the data revealed that the autophagic blockade was not mainly associated with PRE-induced MCF-7 breast cancer cell death.

PRE induces LMP in MCF-7 human breast cancer cells

Considering the close relationship between the autophagic block and lysosomal dysfunction, we then tried to determine the effect of PRE on lysosomal membrane
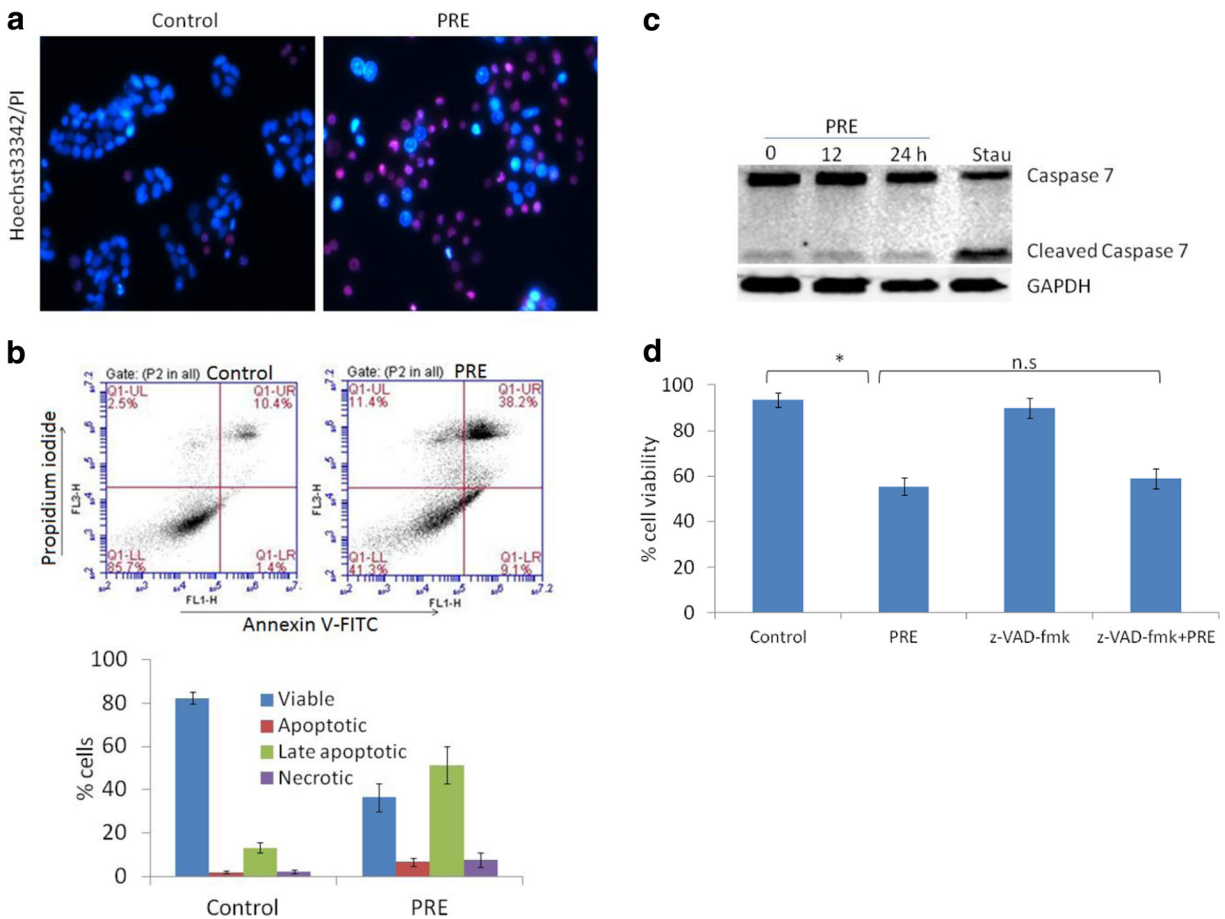
Fig. 2 PRE induces caspase-independent apoptosis-like cell death. **a** To examine the nuclear morphology and plasma membrane integrity, cells were stained with Hoechst 33342 (5 μg/ml) and PI (2 μg/ml). The cells stained with PI showed condensed chromatin, a characteristic of apoptosis. **b** Further, to examine the membrane phosphatidylserine externalization, cells were stained with annexin V-FITC and PI dual staining and analyzed by flow cytometry. The percentage of live, apoptotic, necrotic, and secondary necrotic cells were presented as a graph. **c** Whole cell lysates were subjected to examine the activation of caspase-7 by immunoblotting. **d** Effect of z-VAD-fmk (caspase inhibitor) on PRE-induced cell death. MCF-7 cells were pretreated with z-VAD-fmk (50 μM) for 1 h followed by PRE for 24 h. The percentage cell viability was determined by trypan blue dye exclusion assay using a hemocytometer. Data are representative of three independent experiments. *$P < 0.05$ compared to control group

integrity. LysoTracker probes are fluorescent probes generally used for tracking acidic organelles like lysosomes in live cells. These probes are freely permeable to cell membranes and are typically concentrated in lysosomes. As shown in Fig. 4a, PRE-treated cells showed decreased intensity of LysoTracker Green fluorescence compared to vehicle-treated cells. Also, the cytosolic level of lysosomal protease cathepsin-D was significantly increased in MCF-7 cells treated with PRE (Fig. 4b, c). These observations thus suggest that PRE induces LMP, which then triggers the release of the lysosomal contents into the cytosol. We next investigated whether the loss of lysosomal membrane integrity plays a causative role in PRE-induced breast cancer cell death. For this, we determined the effect of inhibitors against the most abundant lysosomal proteases, cathepsin-B and cathepsin-D, which are the major downstream regulators responsible for induction of cell death following LMP. Unfortunately, both cathepsin inhibitors did not significantly reverse the PRE-induced MCF-7 breast cancer cell death (Fig. 4d).

PRE-induced LMP occurs independent of oxidative stress

Chronic oxidative stress is thought to contribute to the induction of ER stress, LMP, and mitochondrial
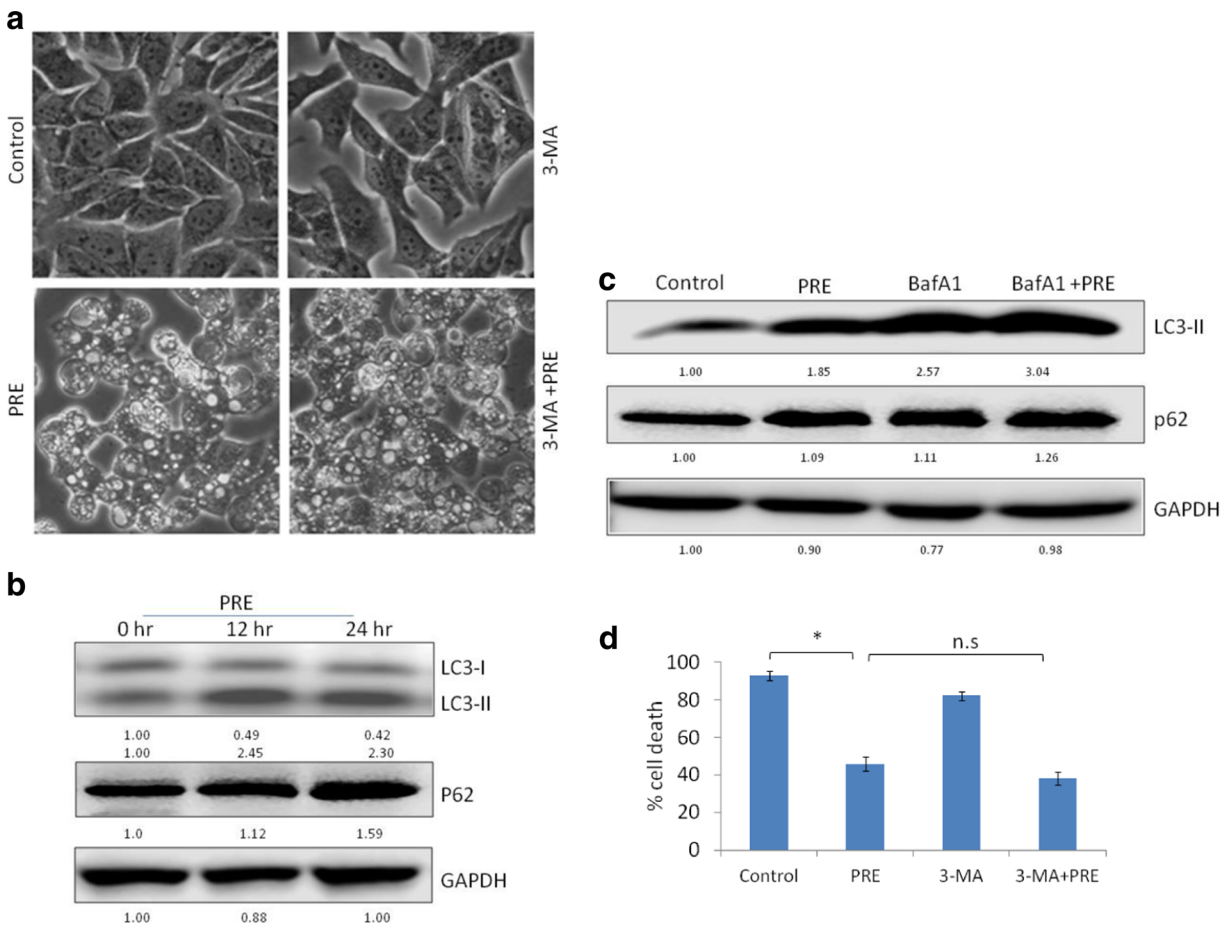
Fig. 3 Effect of PRE on autophagic flux in breast cancer cells. **a** The effect of the autophagic inhibitor 3-MA on PRE-induced cytoplasmic vacuolation. Cells were treated with PRE after 1 h pretreatment with 2 mM of 3-MA. Then, images were captured under a phase-contrast microscope (×200). **b** Determination of the expression of autophagic marker proteins. After 0–24 h treatment with PRE, cells were lysed in CelLytic™ M buffer (Sigma Aldrich) supplemented with protease inhibitor. Equal amounts of proteins were subjected to SDS-PAGE and then immunoblotted for LC3 and p62 proteins. **c** Effect of BafA1 on PRE-induced accumulation of LC3II and p62. MCF-7 cells were pretreated with BafA1 (100 nM) and then with or without PRE. After 24 h, whole cell lysates were prepared and equal amounts of proteins were electrophoresed and immunoblotted. Blots are representative of three independent experiments. **d** The effect of the autophagic inhibitor 3-MA on PRE-induced breast cancer cell death was determined by trypan blue dye exclusion assay using a hemocytometer. Data represent the mean of three independent experiments. *$P < 0.05$ compared to control group

damage, which eventually lead to cell death (Filomeni et al. 2015). Lysosomal membranes are particularly more vulnerable to reactive oxygen species (ROS)-mediated damage because of the lack of an intrinsic antioxidant defense. When ROS production is increased beyond the cellular antioxidant capacity, the excess ROS, hydrogen peroxide in particular, diffuses into the lysosomes, where it reacts with redox-active iron, resulting in the production of hydroxyl radicals. These radicals are highly reactive molecules that destabilize the lysosomal membrane by causing lipid peroxidation as well as damaging lysosomal membrane proteins (Terman et al. 2006). Thus, either chelation of iron or scavenging of ROS can improve lysosomal function (Boya and Kroemer 2008). The iron chelator, deferoxamine, and NAC, an antioxidant, did not significantly inhibit the LMP (Fig. 5a). This was substantiated with the absence of increased ROS production in PRE-treated MCF-7 breast cancer cells (Fig. 5b).
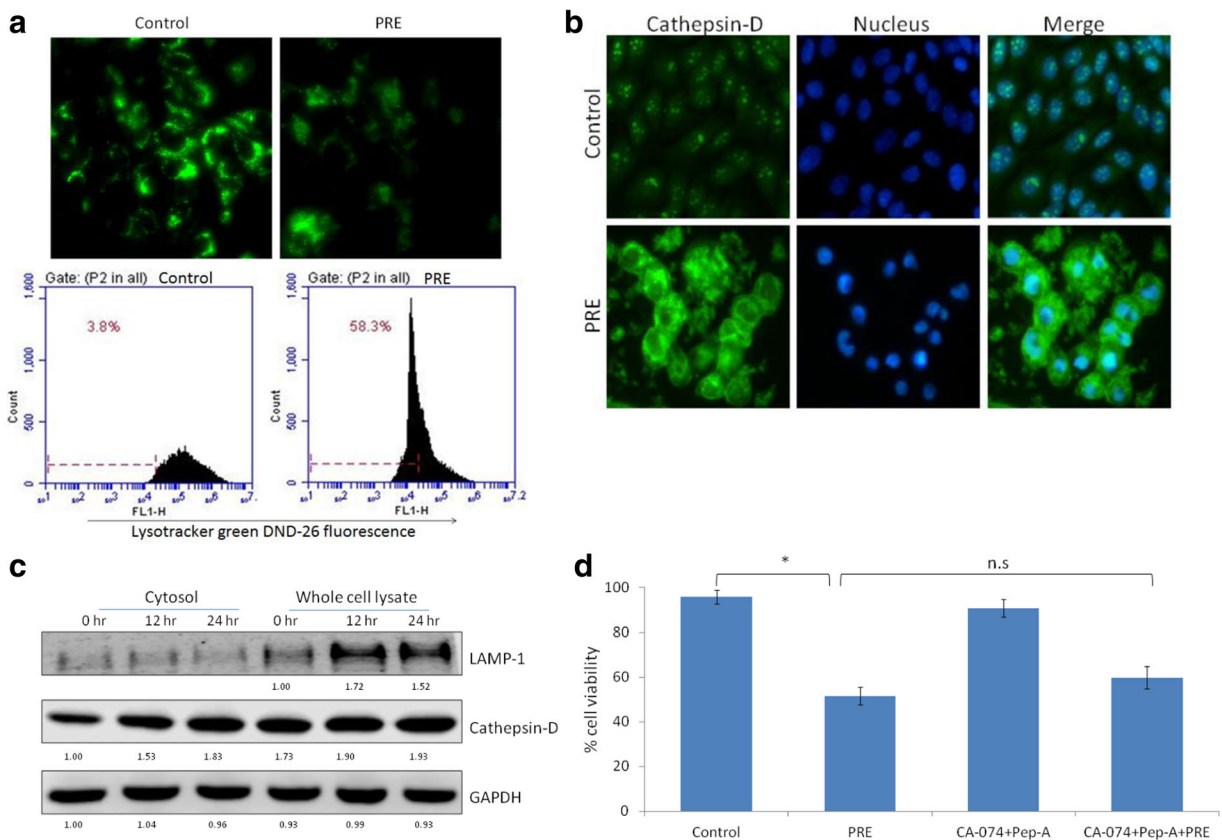
Fig. 4 Effect of PRE on lysosomal membrane integrity in breast cancer cells. **a** MCF-7 cells were plated at a density of 2×10^5 cells per ml in six-well plates. After 24 h treatment with or without PRE, cells were stained with LysoTracker Green DND-26 (100 nM). Then, cells were visualized under fluorescent microscopy and the intensity of LysoTracker Green fluorescence was measured by a flow cytometer. The percentage of decreased fluorescence is indicated in the respective figures. **b** PRE induces cytosolic distribution of cathepsin-D in MCF-7 cells. Cells were seeded on poly-l-lysine-coated coverslips, and after 24 h, cells were treated with PRE. Then, cells were fixed, permeabilized, and subjected to immunostaining of cathepsin-D (green). The nuclei were stained with DAPI, and images were captured under a florescent microscope (×200). **c** PRE induces the leakage of cathepsins from the lysosome to the cytosol. After 0–24 h treatment with PRE, the cytosolic fractions and whole cell lysates were collected and cathepsin-D was detected by western blotting. LAMP-1 was used as a marker for confirming the absence of lysosome contamination. **d** Effect of lysosomal protease inhibitors on PRE-induced cell death. MCF-7 cells were treated with PRE after 1 h pretreatment with CA-074Me and pepstatin-A (10 μM each) for 24 h. Then, cell viability was determined by trypan blue dye exclusion assay. Data are representative of three independent experiments. *$P < 0.05$ compared to control group

Effect of BAPTA-AM (calcium chelator), TPEN (zinc chelator), and geranylgeranylacetone (an inducer of heat shock protein 70 (Hsp70) expression) on PRE-induced LMP

Since dysregulation in calcium homeostasis affects the integrity of various intracellular organelles, including lysosomes, we investigated the influence of calcium depletion on PRE-induced LMP. We pretreated cells with BAPTA-AM for 1 h, then treated the cells with PRE for 24 h, and then analyzed the integrity of the lysosomes. As shown in Fig. 6a, PRE-induced LMP was promoted by the removal of intracellular calcium with BAPTA-AM.

Studies have also shown that intralysosomal accumulation of zinc induces cathepsin-mediated, apoptotic-
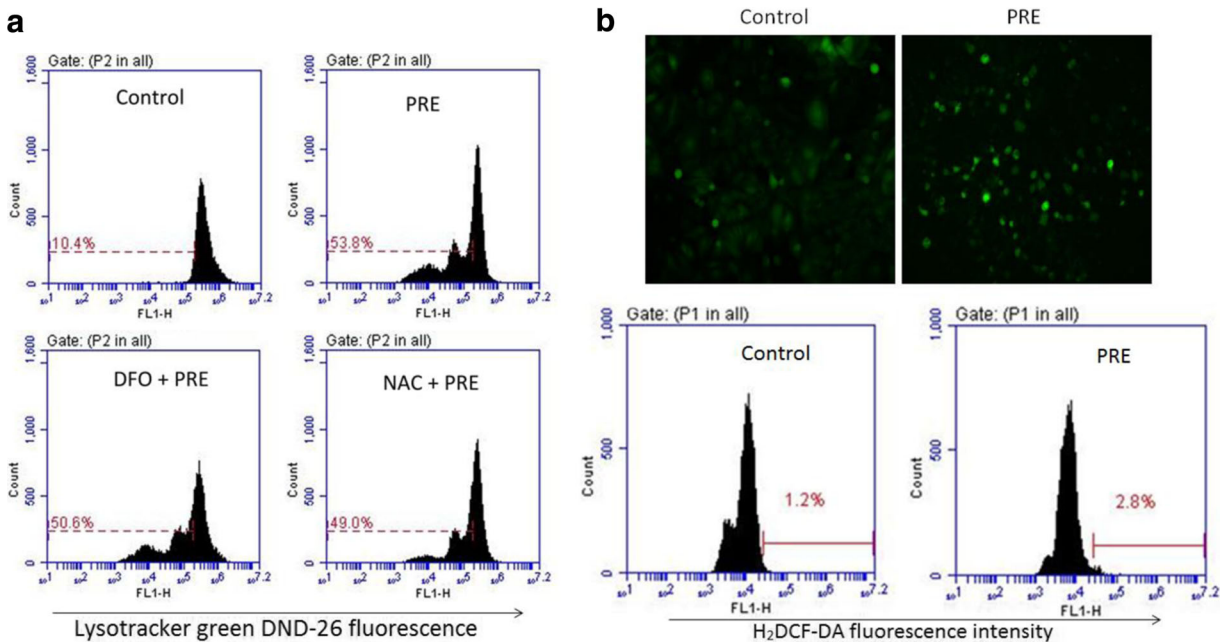
Fig. 5 PRE induces ROS-independent LMP in breast cancer cells. **a** The effect of DFO (100 μM) and NAC (5 mM) on PRE-induced LMP was analyzed by flow cytometry, and then, cells were stained with LysoTracker Green DND-26. The intensity of green fluorescence from 10,000 cells per sample was measured. The percentage number of cells with decreased fluorescence intensity is indicated in the respective figures. **b** ROS determination. Cells were treated with PRE for 24 h and then incubated with 20 μM of H$_2$DCF-DA for 30 min. After washed with PBS, cells were observed and imaged under a fluorescent microscope. The intensity of green fluorescence which is directly proportional to the amount of ROS produced was determined by flow cytometry and the representative data were presented here

like cell death via disruption of lysosomal membrane integrity. To investigate the relationship between intracellular zinc and lysosomal membrane integrity, we examined the effect of a zinc chelator, TPEN, on LMP. Similar to chelation of intracellular calcium, zinc chelation also promotes PRE-induced LMP (Fig. 6a). In addition, Hsp70, an evolutionarily highly conserved, molecular chaperone, plays a vital role in the stabilization of lysosomal membrane integrity. Studies have reported that pharmacological induction of Hsp70 expression inhibits LMP via improving the lysosomal membrane integrity (LeGendre et al. 2015). However, in our study, GGA, an inducer of Hsp70 expression, did not significantly restore the lysosomal membrane integrity in PRE-treated MCF-7 cells (Fig. 6b).

PRE also induces ER stress in MCF-7 breast cancer cells

Next, we found that PRE induces ER stress in MCF-7 cells. Generally, ER stress is resolved by the ER itself, through a self-regulatory UPR mechanism. However,

this mechanism turns into a toxic signal when intense stress persists over a long period of time. The increased fluorescence intensity of ER-Tracker Blue-White DPX dye and the expression of ER stress markers like GRP78, IRE1α, phospho-eIF2α, and CHOP clearly indicate the induction of ER stress in PRE-treated MCF-7 breast cancer cells (Fig. 7a, b).

PRE induces mitochondrial dysfunction in association with lysosomal cathepsins

Following LMP, the lysosomal cathepsins induce apoptotic-like cell death via induction of mitochondrial membrane depolarization. Thus, we first assessed the integrity of the mitochondria using MitoTracker Red. PRE treatment showed significant loss of mitochondrial membrane integrity evidenced from the reduced MitoTracker Red fluorescence intensity compared to untreated control cells (Fig. 8a). The cathepsin inhibitors, CA-074Me and pepstatin-A, demonstrated a significant inhibitory effect on PRE-induced mitochondrial
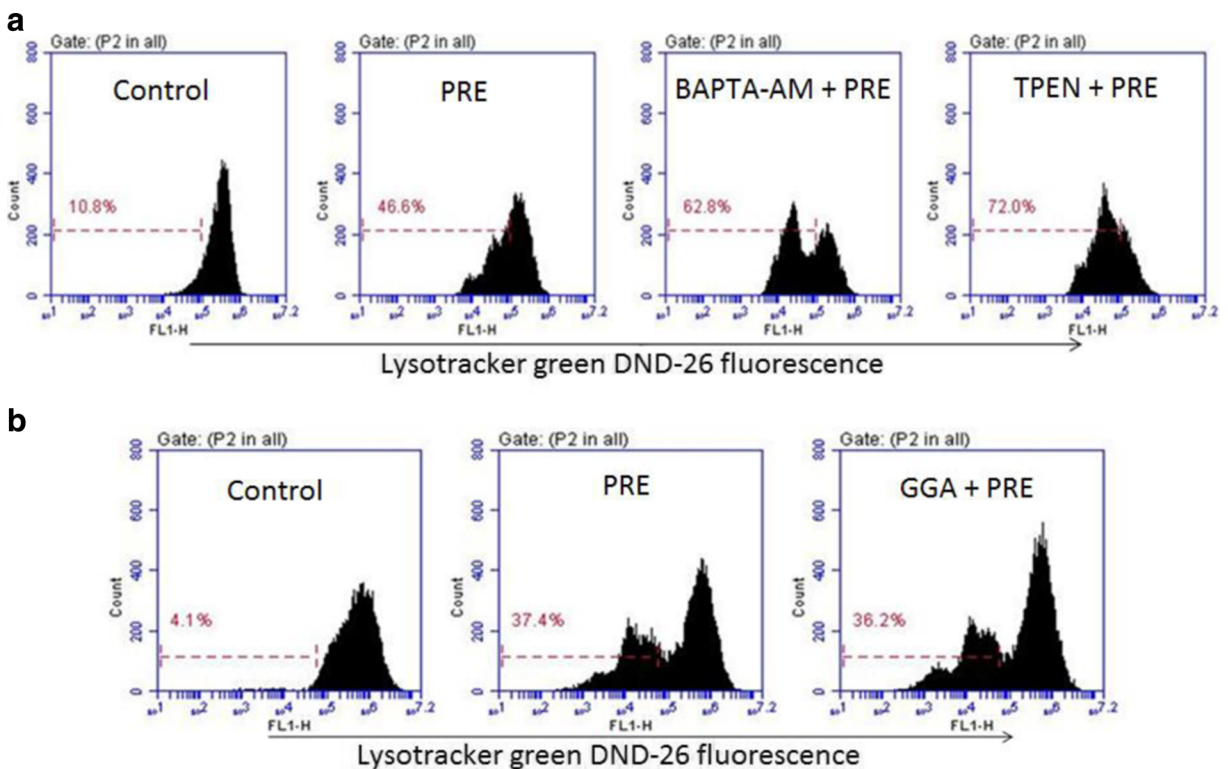
Fig. 6 a Effect of calcium and zinc chelators on PRE-induced LMP in breast cancer cells. MCF-7 cells were pretreated with 20 μM of calcium chelator (BAPTA-AM) or 1 μM of zinc chelator (TPEN) for 1 h, followed by PRE for 24 h. To assess the lysosomal integrity, cells were stained with LysoTracker Green DND-26. Then, the intensity of green fluorescence from 10,000 cells per sample was measured by flow cytometry. The percentage of decreased fluorescence is indicated in the respective figures. b Similarly, the effect of GGA, an inducer of Hsp70 expression on PRE-induced LMP, was analyzed by flow cytometry and the representative data have been presented

damage (Fig. 8b). Further, it is well documented that ER stress-induced cell death is also associated with mitochondrial dysfunction (Song et al. 2016). However, in our study, the ER stress inhibitor 4-PBA failed to restore MMP (Fig. 8c). This may be due to the downstream effects of PRE-induced LMP in MCF-7 cells.

Discussion

The cytotoxicity assay showed that MCF-7 human breast cancer cells were sensitive to PRE in a dose-dependent manner. Furthermore, PRE caused increased accumulation of autophagic marker proteins, LC3 and p62, indicating an incomplete autophagic process in MCF-7 breast cancer cells. Autophagy is an intracellular, lysosomal degradative pathway essential for maintaining cellular homeostasis (Samie and Xu 2014). Thus, any disruption in the lysosomal function could severely impair the autophagic process. In the present study, the decreased

LysoTracker Green fluorescence intensity, as well as the increased cytosolic distribution of the lysosomal protease, cathepsin-D, clearly indicates the loss of lysosomal function. Accordingly, this could be the reason for increased accumulation of autophagosomes in PRE-treated MCF-7 cells. Subsequently, we found that PRE-induced MCF-7 breast cancer cell death was not mainly associated with the autophagic block.

Following LMP, the lysosomal luminal contents are released into the cytosol, setting off indiscriminate degradation of cellular components and thereby promoting cell death. Massive LMP results in apoptotic-like or necrotic cell death without caspase activation, whereas limited LMP can initiate caspase-dependent apoptosis (Boya and Kroemer 2008; Oberle et al. 2010). In the present study, the broad spectrum caspase inhibitor, z-VAD-fmk, did not influence PRE-induced cell death. In addition, Hoechst 33342 and PI, as well as annexin V-FITC and PI, dual staining assays revealed cellular morphological features with characteristics of apoptosis
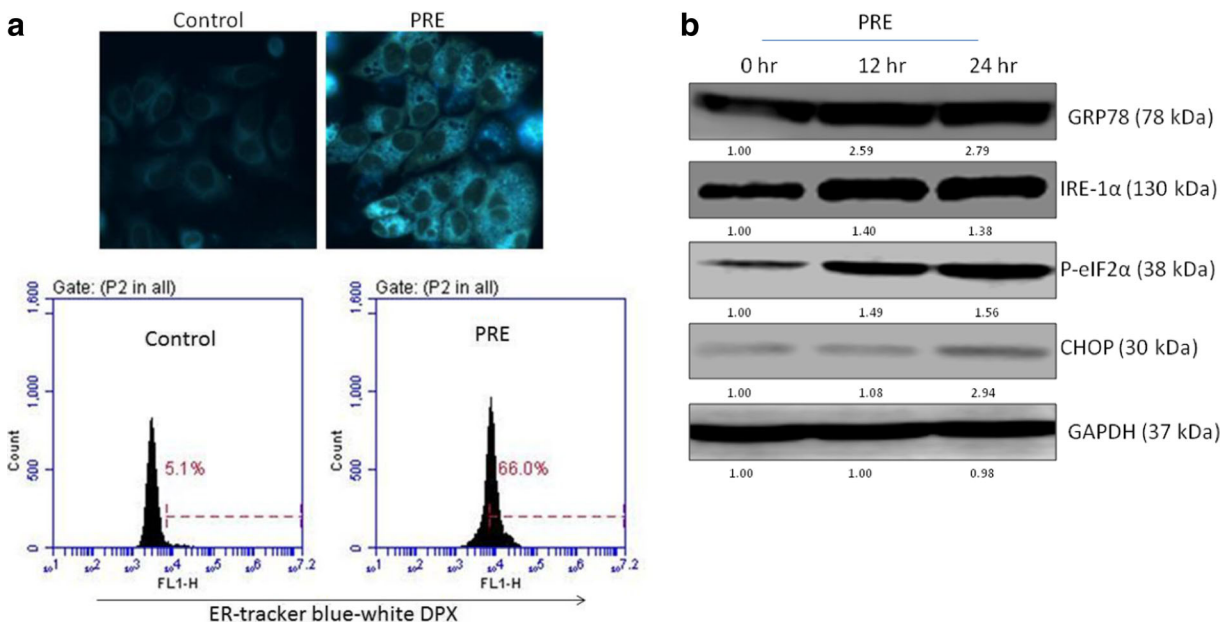
Fig. 7 PRE also induces ER stress in MCF-7 human breast cancer cells. **a** After 24 h treatment with PRE, cells were stained with 1 μM of ER-Tracker Blue-White DPX fluorescence dye for 30 min. The intensity of the ER-Tracker dye was analyzed by fluorescent microscopy as well as flow cytometry. **b** To determine the effect of PRE on ER stress markers, whole cell lysates were subjected to immunoblotting for quantification of GRP78, IRE1α, phospho-eIF2α, and CHOP protein levels. Data are representative of three independent experiments

including chromatin condensation and phosphatidylserine externalization, as well as necrosis in breast cancer cells treated with PRE. These findings evidence the induction of caspase-independent, apoptosis-like cell death by PRE in MCF-7 breast cancer cells. Additionally, PRE-induced MCF-7 breast cancer cell death was fairly influenced by the lysosomal protease inhibitors. Generally, inhibition of the most abundant lysosomal enzymes like cathepsins, that are downstream effectors responsible for induction of cell death following limited LMP, can confer significant protection. However, protection is impossible following extensive LMP due to the lack of inhibition of all of the released lysosomal enzymes without causing massive alterations in cellular functions (Boya and Kroemer 2008).

Several reports clearly demonstrate that phenolic compounds induce cytotoxicity via increasing the production of cellular ROS. Cellular ROS are a group of molecules that influence various signal transduction pathways and perform critical functions in cells (Covarrubias et al. 2008; Zuo et al. 2015). Oxidative stress occurs when production of ROS overwhelms the cellular antioxidant defense or when there is a decrease in the cellular antioxidant capacity (Poljsak et al. 2013). ROS can induce LMP indirectly by reacting with intralysosomal iron, which produces the highly reactive hydroxyl radicals through the Fenton reaction (Terman et al. 2006). Here, we found that both deferoxamine (iron chelator) and *n*-acetylcysteine (antioxidant) failed to improve the lysosomal integrity in PRE-treated cells. This data represents the involvement of an oxidative stress-independent mechanism in PRE-induced LMP in MCF-7 breast cancer cells. Hsp70 is an evolutionarily highly conserved molecular chaperone which is localized on the lysosomal membrane that protects against LMP by promoting acid-sphingomyelinase activity and stabilizing the interaction between acid-sphingomyelinase and bis(monoacylglycero)phosphate (Nylandsted et al. 2004). Nylandsted et al. (2000) have reported that the downregulation of Hsp70 induces caspase-independent cell death in breast cancer cells. Hence, overexpression of Hsp70 is thought to promote lysosomal integrity. In the present study, pharmacological induction of Hsp70 expression with GGA showed no significant improvement of the lysosomal integrity in MCF-7 breast cancer cells.

Moreover, another possibility is that impaired zinc and calcium homeostasis also greatly influence the integrity of lysosomes (Lee and Koh 2010; Rodríguez-Muela et al. 2015). Zinc is an indispensable
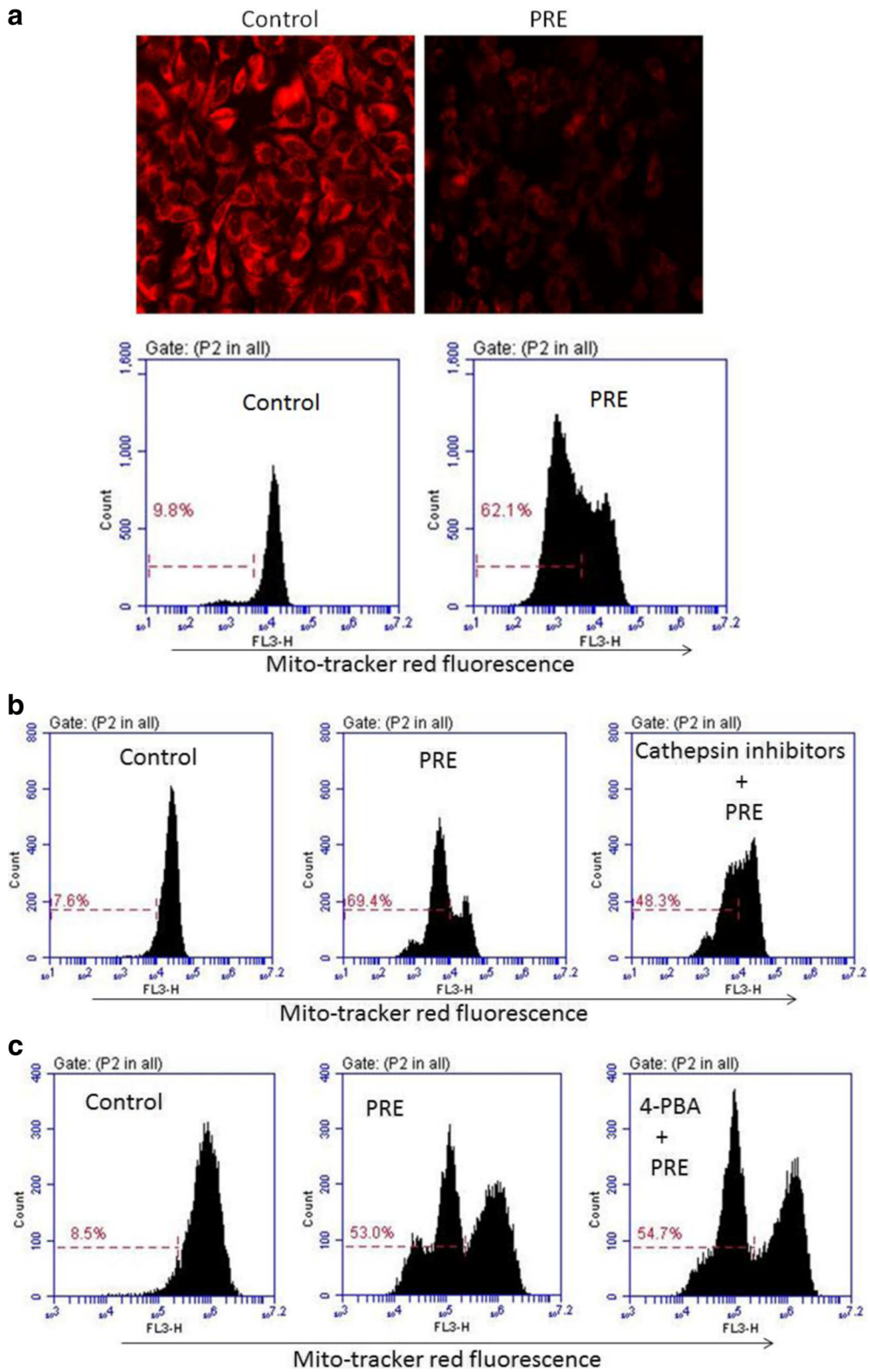
◀ **Fig. 8** PRE damages mitochondrial membrane integrity in MCF-7 cells. **a** After treatment with PRE, cells were stained with MitoTracker Red (200 nM). Then, images were captured under a fluorescent microscope and the intensity of the dye was quantified by flow cytometry. **b** Effect of cathepsin inhibitors on PRE-induced mitochondrial membrane damage. First, cells were pretreated with the inhibitors CA-074Me and pepstatin-A (10 μM each) for 1 h, followed by 24 h treatment with PRE. Then, the mitochondrial membrane integrity was analyzed by flow cytometry and then cells were stained with MitoTracker Red. **c** Likewise, the effect of ER stress inhibitor, 4-PBA (2 mM), on mitochondria was analyzed by flow cytometry using MitoTracker Red. Data are representative of three independent experiments

micronutrient that regulates many cellular functions. Though zinc accumulates in virtually all cellular organelles, lysosomes play a vital role in maintaining the intracellular labile zinc concentration, as they absorb zinc from the cytosol. Generally, zinc is essential for lysosomal acidification and exocytosis (Kukic et al. 2014). However, abundance of cellular zinc levels has been linked to catastrophic consequences, like loss of lysosomal membrane integrity (Kukic et al. 2014). Likewise, increased intracellular accumulation of calcium could induce LMP by targeting the molecules responsible for lysosomal membrane integrity like lysosomal-associated membrane protein 2a (LAMP2a) via activation of calpains (Villalpando Rodriguez and Torriglia 2013). A clinically used alcohol-deterrent disulfiram induces LMP in breast cancer cells by increasing the lysosomal sequestration of zinc. Additionally, the well-known, extensively studied anticancer phenolic compound, curcumin, induces lysosomal destabilization by increasing intracellular calcium in human hepatocarcinoma cells (Wiggins et al. 2015; Moustapha et al. 2015). Here in our study, depletion of intracellular zinc and calcium using specific chelators promotes the PRE-induced LMP in MCF-7 cells.

Further, we observed that PRE induces ER stress in MCF-7 breast cancer cells. Studies have reported that lysosomal dysfunction can induce ER stress by increasing the accumulation of ubiquitinated proteins (Yu et al. 2013). So, the stress to the ER in PRE-treated MCF-7 cells may be due to the loss of lysosomal function. Following LMP, the lysosomal cathepsins can directly promote mitochondrial membrane depolarization (Boya and Kroemer 2008). Likewise, ER stress can also induce mitochondrial membrane damage via its downstream effectors, in order to cause apoptotic cell death (Lee et al. 2010). Here, inhibition of cathepsins using chemical inhibitors showed significant protective effects on mitochondrial membrane integrity. However, the ER stress inhibitor, 4-PBA, did not significantly influence the effect of PRE on mitochondrial damage. We speculate that 4-PBA fails to preserve mitochondrial membrane potential due to the downstream effects of LMP in PRE-treated MCF-7 cells.

Conclusion

The results suggest that PRE-induced cytoplasmic vacuolation in MCF-7 cells might be due to lysosomal and ER dilation as well as accumulation of autophagosomes. The loss of these vital organelles integrity and mitochondrial membrane depolarization might be partly responsible for PRE-induced caspase-independent, apoptosis-like cell death in MCF-7 human breast cancer cells. However, more studies are warranted to explore the mechanism behind PRE-induced MCF-7 human breast cancer cell death.

References

Aits S, Jäättelä M. Lysosomal cell death at a glance. J Cell Sci. 2013;126(Pt 9):1905–12.

Amelio I, Melino G, et al. Cell death pathology: cross-talk with autophagy and its clinical implications. Biochem Biophys Res Commun. 2011;414(2):277–81.

Apel A, Herr I, et al. Blocked autophagy sensitizes resistant carcinoma cells to radiation therapy. Cancer Res. 2008;68(5):1485–94.

Appelqvist H, Wäster P, et al. The lysosome: from waste bag to potential therapeutic target. J Mol Cell Biol. 2013;5(4):214–26.

Bjørkøy G, Lamark T, et al. Monitoring autophagic degradation of p62/SQSTM1. Methods Enzymol. 2009;452:181–97.

Boya P, Kroemer G. Lysosomal membrane permeabilization in cell death. Oncogene. 2008;27(50):6434–51.

Chen X, Li Y, et al. Tea polyphenols induced apoptosis of breast cancer cells by suppressing the expression of survivin. Sci Rep. 2014;4:4416.

Covarrubias L, Hernández-García D, et al. Function of reactive oxygen species during animal development: passive or active? Dev Biol. 2008;320(1):1–11.

Filomeni G, De Zio D, et al. Oxidative stress and autophagy: the clash between damage and metabolic needs. Cell Death Differ. 2015;22(3):377–88.

Hasima N, Ozpolat B. Regulation of autophagy by polyphenolic compounds as a potential therapeutic strategy for cancer. Cell Death Dis. 2014;5:e1509.

Heymann D. Autophagy: a protective mechanism in response to stress and inflammation. Curr Opin Investig Drugs. 2006;7(5):443–50.

Howell A. An early peak of relapse after surgery for breast cancer. Breast Cancer Res. 2004;6(6):255–7.

Klionsky DJ, Elazar Z, et al. Does bafilomycin A1 block the fusion of autophagosomes with lysosomes? Autophagy. 2008;4(7):849–50.

Komatsu M, Ichimura Y. Physiological significance of selective degradation of p62 by autophagy. FEBS Lett. 2010;584(7):1374–8.

Kukic I, Kelleher SL, et al. Zn2+ efflux through lysosomal exocytosis prevents Zn2+-induced toxicity. J Cell Sci. 2014;127(Pt 14):3094–103.

Lee SJ, Koh JY. Roles of zinc and metallothionein-3 in oxidative stress-induced lysosomal dysfunction, cell death, and autophagy in neurons and astrocytes. Mol Brain. 2010;3(1):30.

Lee JW, Kim WH, et al. ER stress is implicated in mitochondrial dysfunction-induced apoptosis of pancreatic beta cells. Mol Cells. 2010;30(6):545–9.

LeGendre O, Breslin PA, et al. (−)-Oleocanthal rapidly and selectively induces cancer cell death via lysosomal membrane permeabilization. Mol Cell Oncol. 2015;2(4):e1006077.

Livesey KM, Tang D, et al. Autophagy inhibition in combination cancer treatment. Curr Opin Investig Drugs. 2009;10(12):1269–79.

Mena S, Rodríguez ML, et al. Pterostilbene-induced tumor cytotoxicity: a lysosomal membrane permeabilization-dependent mechanism. PLoS One. 2012;7(9):e44524.

Moustapha A, Pérétout PA, et al. Curcumin induces crosstalk between autophagy and apoptosis mediated by calcium release from the endoplasmic reticulum, lysosomal destabilization and mitochondrial events. Cell Death Dis. 2015, Article number: 15017.

Nylandsted J, Rohde M, et al. Selective depletion of heat shock protein 70 (Hsp70) activates a tumor-specific death program that is independent of caspases and bypasses Bcl-2. Proc Natl Acad Sci U S A. 2000;97(14):7871–6.

Nylandsted J, Gyrd-Hansen M, et al. Heat shock protein 70 promotes cell survival by inhibiting lysosomal membrane permeabilization. J Exp Med. 2004;200(4):425–35.

Oberle C, Huai J, et al. Lysosomal membrane permeabilization and cathepsin release is a Bax/Bak-dependent, amplifying event of apoptosis in fibroblasts and monocytes. Cell Death Differ. 2010;17(7):1167–78.

Ostenfeld MS, Fehrenbacher N, et al. Effective tumor cell death by sigma-2 receptor ligand siramesine involves lysosomal leakage and oxidative stress. Cancer Res. 2005;65(19):8975–83.

Poljsak B, Šuput D, et al. Achieving the balance between ROS and antioxidants: when to use the synthetic antioxidants. Oxid Med Cell Longev. 2013;2013:956792.

Racoma IO, Meisen WH, et al. Thymoquinone inhibits autophagy and induces cathepsin-mediated, caspase-independent cell death in glioblastoma cells. PLoS One. 2013;8(9):e72882.

Rodríguez-Muela N, Hernández-Pinto AM, et al. Lysosomal membrane permeabilization and autophagy blockade contribute to photoreceptor cell death in a mouse model of retinitis pigmentosa. Cell Death Differ. 2015;22(3):476–87.

Samie MA, Xu H. Lysosomal exocytosis and lipid storage disorders. J Lipid Res. 2014;55(6):995–1009.

Sano R, Reed JC. ER stress-induced cell death mechanisms. Biochim Biophys Acta. 2013;1833(12):3460–70.

Song Q, Gou WL, et al. FAM3A attenuates ER stress-induced mitochondrial dysfunction and apoptosis via CHOP-Wnt pathway. Neurochem Int. 2016;94:82–9.

Suganuma M, Kurusu M, et al. Green tea polyphenol stimulates cancer preventive effects of celecoxib in human lung cancer cells by upregulation of GADD153 gene. Int J Cancer. 2006;119(1):33–40.

Terman A, Kurz T, et al. Lysosomal labilization. IUBMB Life. 2006;58(9):531–9.

Trondl R, Flocke LS, et al. Triapine and a more potent dimethyl derivative induce endoplasmic reticulum stress in cancer cells. Mol Pharmacol. 2014;85(3):451–9.

Villalpando Rodriguez GE, Torriglia A. Calpain 1 induce lysosomal permeabilization by cleavage of lysosomal associated membrane protein 2. Biochim Biophys Acta. 2013;1833(10):2244–53.

Wei T, Kang Q, et al. Activation of autophagy and paraptosis in retinal ganglion cells after retinal ischemia and reperfusion injury in rats. Exp Ther Med. 2015;9(2):476–82.

Weng CJ, Yen GC. Chemopreventive effects of dietary phytochemicals against cancer invasion and metastasis: phenolic acids, monophenol, polyphenol, and their derivatives. Cancer Treat Rev. 2012;38(1):76–87.

Wiggins HL, Wymant JM, et al. Disulfiram-induced cytotoxicity and endo-lysosomal sequestration of zinc in breast cancer cells. Biochem Pharmacol. 2015;93(3):332–42.

Wu YT, Tan HL, et al. Dual role of 3-methyladenine in modulation of autophagy via different temporal patterns of inhibition on class I and III phosphoinositide 3-kinase. J Biol Chem. 2010;285(14):10850–61.

Yadav RK, Chae SW, et al. Endoplasmic reticulum stress and cancer. J Cancer Prev. 2014;19(2):75–88.

Yu C, Huang X, et al. Lysosome dysfunction enhances oxidative stress-induced apoptosis through ubiquitinated protein accumulation in Hela cells. Anat Rec (Hoboken). 2013;296(1):31–9.

Zuo L, Zhou T, et al. Biological and physiological role of reactive oxygen species—the good, the bad and the ugly. Acta Physiol (Oxf). 2015;214(3):329–48.